Digital Extraction of Altitudinal Belt Spectra in the West Kunlun Mountains Using SPOT-VGT NDVI and SRTM DEM

XIAO Fei[*], LING Feng, DU Yun, XUE Huaiping, and WU Shengjun

Institute of Geodesy & Geophysics, Chinese Academy of Sciences, Wuhan 430077, China

[*] Corresponding author, e-mail: xiaof@whigg.ac.cn; Tel: 86-27-68881901; Fax: 86-27-68881362

Abstract: In this paper, a digital identification method for the extraction of altitudinal belt spectra of montane natural belts is presented. Acquiring the sequential spectra of digital altitudinal belts in mountains at an acceptable temporal frequency and over a large area requires extensive time and work if traditional methods of field investigation are to be used. Such being the case, often the altitudinal belts of a whole mountain or the belts at a regional scale are represented by single points. However, single points obviously cannot accurately reflect the spatial variety of altitudinal belts. In this context, a digital method was developed to extract the spectra of altitudinal belts from remote sensing data and SRTM DEM in the West Kunlun Mountains. By means of the 1km resolution SPOT-4 vegetation 10-day composite NDVI, the horizontal distribution of altitudinal belts were extracted through supervised classification, with a total classification accuracy of 72.23%. Then, a way of twice-scan was used to realize the automatic transition of horizontal maps to vertical belts. The classification results of remote-sensing data could thus be transformed automatically to sequential spectra of digital altitudinal belts. The upper and lower lines of the altitudinal belts were then extracted by vertical scanning of the belts. Relationships between the altitudinal belts based on the montane natural zones concerning vegetation types and the geomorphological altitudinal belts were also discussed. As a tentative method, the digital extraction method presented here is effective at digitally identifying altitudinal belts, and could be helpful in rapid information extraction over large-scale areas.

Key words: Altitudinal belt spectra; Kunlun Mountains; NDVI; Digital extraction

Introduction

Mountains are important and complex ecological systems of the global system, characterized by a high degree of diversity in climate and landscape (Zhang et al. 2006). Because of their complicated topography, the spatial distributions of temperature, precipitation, vegetation, soil, etc. in mountains are very different over short horizontal distances (Kuhle 2007). This generates tremendous habitat and species diversity (FENG et al. 2006). Ecological systems in mountain regions are very sensitive to changes in climate, weather patterns and human activities, and are thus important for environmental change research.

Altitudinal zonality is one of the most outstanding spatial patterns of ecological environment in mountains (Troll 1972). As a manifestation of altitudinal zonality, altitudinal belts are a kind of geographic distribution area

delimited by altitude-related environmental constraints (ZHANG et al. 2003). Both upper and lower boundaries of the altitudinal belt represent a tension zone, where species reach a distribution limit. Considering that mountain regions may experience the impacts of the rapidly changing global environment more strongly than other regions (ZHONG 2000), altitudinal belts with vertical distributions of species may change markedly during global change (Becker and Bugmann 1999) and may be sensitive indicators of subsequent environmental impacts to lowlands.

Not only at the valley scale, but also at the global scale, all changes to altitudinal belts, such as the snowline and tree line, are important geographic elements in evaluating the effects of environmental change (Körner 1998, Guglielmin et al. 2003, Kullman and Kjallgren 2006, Schweizer and Kronholm 2007), and have received much attention. Altitudinal belts have long been the basic research units in the study of mountain regions (HUANG 1962, ZHONG 2000). The earliest related research of altitudinal zonality can be traced back to the 19th century, when Alexander von Humboldt studied the Andes Mountains (ZHANG et al. 2003). In general, different phases have different emphases in altitudinal belt studies. Comparison of altitudinal belts among different mountains began in the 1930s (Troll 1972). After that, the relationship between altitudinal zonality and horizontal zonality was studied in the 1960s (JIANG 1964, HUANG 1962). Quantitative analysis was introduced to altitudinal belt study after the 1970s (Troll 1972, NIU 1980, Allan 1986), and the relationships between moisture, heat and the spatial patterns of altitudinal belts were quantified in some mountains (HOU 1980, LIU 1981, ZHENG et al. 1984, PENG et al. 1999). Following the progress of GIS, digital visualization, integration and comparison of altitudinal belts are currently hotly debated issues in mountain altitudinal belt research (ZHANG et al 2006, ZHANG 2008).

The concept of altitudinal zones was originally based on vegetation changes at different altitudes in high mountains and can be dated back to the ideas of Von Humboldt (Böse 2006). Many scientists subsequently generalized multiple spectrum systems of altitudinal belts in different areas based on their own knowledge and investigations. Nowadays there are many classification systems for altitudinal belts, the main systems being those based on vegetation zones, soil zones, geomorphologic zones, eco-geographic types and climatic zones, etc (ZHANG et al. 2004). Obviously, different altitudinal belt systems are defined in different ways. In this paper, we adopted the system of altitudinal belts based on the montane natural zones concerning vegetation types developed by ZHANG Baiping (2003). This system is a three-level system of digital spectra and includes 31 basic spectrum series and seven peculiar spectrum series. This classification system is an integrated frame which is able to include all the types and spatial patterns of Chinese mountain altitudinal belts.

The study of altitudinal belts calls for more systemic spatial-temporal data, especially spatial continuous data. However, since there are only very limited data for some mountains, it is not enough to demonstrate vertical vegetation zonation. For some mountains there are virtually no data (ZHANG et al. 2006). Traditionally, altitudinal belt data have been ascertained from field surveys (ZHENG et al. 1984, ZHENG 1994, PENG et al. 1997). Field surveys can provide accurate information about the limit elevations of different belts along the survey routes, but take much time and effort. Field surveys cannot provide the spatial patterns of altitudinal belts on a large scale too. Accordingly, there are still data limitations and incomplete information on the spatial distributions of altitudinal belts (ZHONG 2000, ZHANG 2008). Such being the case, the altitudinal belts of a whole mountain or the belts at a regional scale are often represented by single points. Obviously, single points cannot reflect the spatial variety of altitudinal belts accurately. Therefore, it is still difficult to rapidly acquire or update continuous altitudinal belts over large areas. In this context, the key objective of this research effort was to develop a method which can be used to digitally extract sequential spectra of altitudinal belts from remotely sensed data.

1 Methods

As is well known, both remotely sensed images and vegetation maps provide useful and spatially continuous land cover information on a large scale.

However, both are horizontally distributed, while altitudinal belts are vertically distributed (ZHANG et al. 2003). As a result, horizontally-distributed data are seldom used to analyze the patterns of the altitudinal belts. In spite of the fact that horizontal data are different from the frame of altitudinal belts, the abundant land cover information contained in vegetation maps and remotely sensed images is an important data source for altitudinal belts (XIAO 2006). In this paper, a method based on the spatial analysis of GIS was developed to extract the continuous spatial distribution of altitudinal belts from remotely sensed images. The study was conducted in the West Kunlun Mountains.
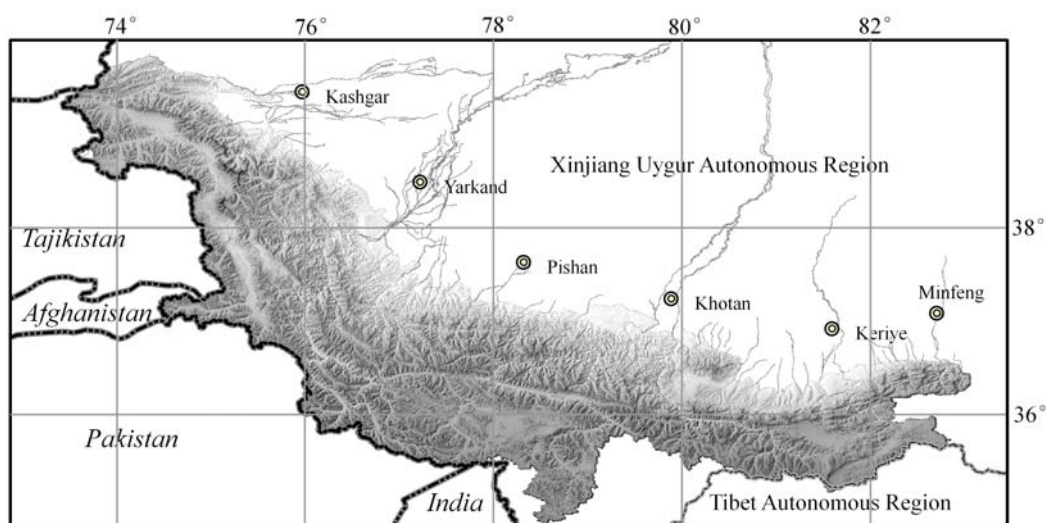
1.1 Study area

The study area, the West Kunlun Mountains, is located in northwest China at approximately 35° - 40° N and 73° - 84° E, and is characterized by distinct topography and an arid climate. It extends from the Pamirs, run eastwards along the northern part of the Tibetan plateau, and stretches along the southern edge of Tarim Basin (as shown in figure 1). The heights of the mountains in the study area commonly exceed 6000m. Consequently, altitudinal belts are very distinct in the West Kunlun Mountains. According to the geographic location, altitudinal belts in this area belong to the system of mid-latitude continental altitudinal belts.

Based on the data of previous field investigations (ZHENG 1999, ZHANG et al. 2003), altitudinal belts in this area are made up of nival belt, sub-nival belt, alpine desert belt, alpine meadow, alpine steppe, montane forest-steppe belt, montane steppe belt, montane steppe-desert belt, montane desert, etc. Altitudinal belts are often quite disparate on different exposures of the same mountain (ZHENG and GAO 1984, ZHENG 1999). From west to east, the altitudinal belts of the Kunlun Mountains change according to a unique model called the structure-thinning model (ZHANG et al. 2003). In general, the patterns and the changes in altitudinal belts are the most outstanding environmental characteristics in this area.

1.2 Remote sensing and accuracy assessment of altitudinal belts

Although field investigations can provide accurate information related to altitudinal belts, they are time-consuming and difficult to carry out on a large scale. With rapid progress from qualitative to quantitative, the technology of Remote Sensing (RS) has been widely used in environment monitoring. At present, remotely sensed images have already proven useful as a data source for vegetation mapping. However, very few previous studies directly on the remote sensing of altitudinal belts have been published. Related

Figure 1 Location and boundary of the study area

works are mainly concentrated on the vegetations response to environmental conditions along altitudinal zone using remote sensing technique (Hill et al. 2007, Olthof and Pouliot 2010).

Time series of vegetation indices have been used for decades as a measure of vegetation photosynthetic activity (Schmidt and Karnieli 2000, WANG and Tenhunen 2004, Lunetta et al. 2006). Considering that vegetation is the most important indicator in the classification of altitudinal belts, and that time series of the Normalized Difference Vegetation Index (NDVI) can separate different land cover types based on their phenology or seasonal signal (ZHOU et al. 2001, Weiss et al. 2004), NDVI was used to extract the information of vegetation distribution and, from that, the altitudinal belts. As NDVI from SPOT-4 VGT data is considered an improvement over AVHRR (Advanced Very High Resolution Radiometer) NDVI, the 1km resolution SPOT-4 vegetation 10-day composite NDVI (SPOT-4 VGT-S10 NDVI) data was selected to monitor vegetation in the study area.

The SPOT-4 VGT instrument is a large field of view optical sensor designed for observations of vegetation and land surfaces onboard the SPOT-4 earth observation satellite system. The VGT instrument has four spectral bands from 460 nm to 1.67μm with the absolute calibration accuracy of spectral about 5% and geometric accuracy less than 0.3 pixels (Jarlan 2008). It provides daily global coverage data at 1km spatial resolution. The VGT-S10 NDVI products are generated from the physical products which are atmospherically corrected for molecular and aerosol scattering, water vapor, ozone and other gas absorption (Fensholt et al 2009), and then synthesized by a Maximum Value Compositing (MVC) procedure to ensure coverage of landmasses with a minimum effect of cloud cover per 10 days. Cloud removing, atmospheric correction, and bi-directional compositing procedures substantially reduce the noise in NDVI at the time of imaging (Tarnavsky 2008).

In order to catch the differences in seasonal phenology among belts, and classify the different belts effectively, the whole series of SPOT-4 VGT-S10 NDVI over one year were all joined for belt extraction. The NDVI data were distributed by VITO at http://free.vgt.vito.be/. The initial NDVI images were scaled from their original 10-bit format to 8-bit images (0-255) which are more convenient to be used on 8-bit gray tone displays. Image rectification and geo-processing were conducted using ERDAS Imagine 8.7 image processing software. Statistical analysis of the relationships between the NDVI values and time was carried out for different types of altitudinal belts according to sampling points from previous field investigations and the Vegetation Atlas of China (1:1 000, 000) (HOU 2001). This vegetation atlas is the most detailed and accurate vegetation map of the study area at present. In order to ensure the time consistency between the atlas and remotely sensed images, the NDVI data of 2000 were selected here. Figure 2 shows the scaled NDVI-responses per 10 days in the course of 2000 for the nine types of altitudinal belts. The curves
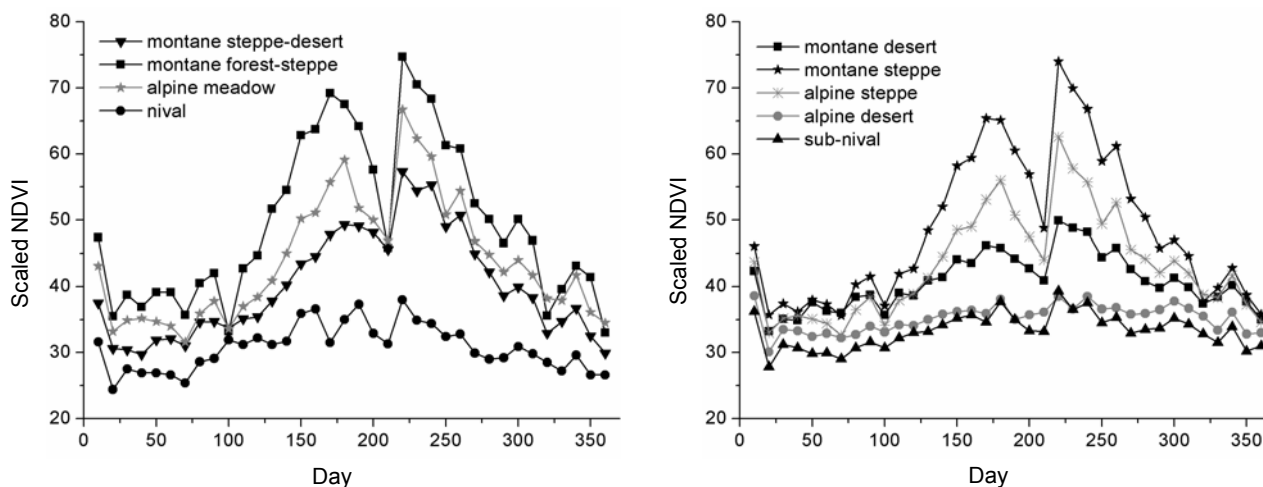

Figure 2 NDVI-responses per 10 days in the course of 2000 for the nine types of altitudinal belts

are correspondent well with the natural phenomena of the altitudinal belts phenologys. The scaled NDVI values of Montane forest-steppe and montane steppe are higher than other belts. Although there are abnormal fluctuations in NDVI values from July to August, the different seasonal signals among altitudinal belts are discernible and adequate for classifying the altitudinal belts.

There are several methods for the analysis of time series NDVI images, such as cluster analysis and principal component analysis (PCA). PCA was used in this paper to compress the series of NDVI data into a smaller number of principal component image bands which contain most of the statistical variances of the original input image. Then a supervised classification was performed on these data. Supervised classification clusters the image pixels into classes according to user-defined training classes.

From selecting the homogenous areas for each of the desired classification categories, a vector layer which consists of various polygons overlaying different altitudinal belt types was digitized over the raster images. Thus the training data was gathered manually here via prior experiences. Among different decision rules which can be applied in a supervised classification methodology, here we selected the parametric rule of Maximum Likelihood in the classification. When the training data was input into the classifier, the mean spectral signature for each class was calculated. The entire image was then classified based on the training data metrics using approved feature sets and the maximum likelihood method. Afterwards, classification result was sieved and then clumped to remove some noises in the image.

For the last result of classification, there would be an accuracy assessment from the Kappa coefficient. The Vegetation Atlas of China (1:1 000 000) (HOU 2001) was used here as the reference data, and the data used in accuracy assessment came from random sampling.

1.3 Digital extraction of the altitudinal belts

In order to analyze the spatial pattern of altitudinal belts in mountains, an extension direction of continuous spectra, such as the orientation of mountain strike, longitude or latitude, is often prescheduled as the abscissa

(ZHANG et al. 2006), Since the West Kunlun Mountains ranges from west to east, and their strike direction is almost identical to latitude, latitude direction was chosen as the prescheduled direction to carry out the altitudinal belt extraction. As the altitudinal belts of the adret are often quite different from those of the ubac, here we take only the adret of the Kunlun Mountains as an example.

1.3.1 Geographic unit partition

To fix the exact boundary of altitudinal belts in this study, an accurate ridge line dividing the southern slopes of the West Kunlun Mountains from the northern slopes should first be ascertained. A scheme of geomorphology unit dividing was presented in the treatise "Physical geography of the Karakorum-Kunlun Mountains" (ZHENG 1999). Referenced with the existing dividing scheme, the Shuttle Radar Topography Mission (SRTM) Digital Elevation Model (DEM) of the study area was then applied to extract an accurate dividing ridge line.

The SRTM DEM is one of the most accurate near-global elevation data covering continental areas from 60° N to 56° S with a 1-arc sec ($\approx$ 30m) and 3-arc sec ($\approx$ 90m) spatial resolution. The 3-arc sec data are publicly available, while 1-arc sec data are only for the United States. Thus we used 3-arc sec data here. According to the mission objectives of SRTM, the absolute horizontal circular accuracy requirement was 20m, and the requirement for absolute vertical accuracy and relative vertical accuracy was less than 16m and 10m respectively for 90% of the data (Rabus et al. 2003, Luedeling et al. 2007). From performance evaluations by SRTM project team, the German Aerospace Center (DLR) and some other organizations, it was proved that the SRTM data meets the requirements (Rodriguez et al. 2006, Rabus et al. 2003, Smith and Sandwell 2003). Since the variance ranges of altitudinal belt boundaries are far greater than the biases of SRTM data, the accuracy of the SRTM DEM is sufficient for altitudinal belt extraction. However, SRTM data often contains some data voids in mountain areas because of radar shadowing. These would lead to some errors in the results of altitudinal belts extraction. For the data voids, we simply replaced no data cells with 1:250,000 DEM of the study area.

Many hydrologic analysis functions are

presently available in GIS. The hydrologic analysis extension in ArcGIS provided a method to characterize the drainage areas. The first step was to determine the direction of flow from every cell in the input grid. Sinks in the DEM may result in an erroneous flow-direction grid in the flow direction process, so we should identify and fill the sinks using the Spatial Analyst ZonalFill function. Then we can obtain a depressionless DEM. After this, a grid of accumulated flow to each cell should be created by accumulating the weight for all cells that flow into each downslope cell with the Flowaccumulation function. Afterwards, based on the calculated direction raster and the accumulation raster, the study area could be divided into sub-watersheds using the Wastershed function. Then the borderline of sub-watersheds on the north side of the Kunlun Mountains could be identified, grouped and shaped into ridge lines according to the referenced dividing scheme.

1.3.2 Belt boundary calculation

Although the horizontal edge of adret was delimitated through geographic unit partition, it was different with the altitudinal spectra boundary. Due to the 2-dimension vertical structure of the altitudinal belt, the highest limit of altitudinal belts should be made up of continuous boundary lines of the mountaintop, and the lowest limit of altitudinal belts should consist of the lowest points in this area. Accordingly, the silhouette line of the mountains in the NS-trending could be seemed as the bound of altitudinal belts, and thus it should be extracted before belts extraction. In this paper, a method was presented to extract the edge lines. Firstly, the DEM of the study area was scanned with a beam of parallel line which is along the vertical direction to the ground. Then, the highest point among the intersection point in every beam could be recorded. All of the highest points would be recorded when the DEM was scanned over by the parallel beam from west to east. Eventually, the extracted points would form a continuous border line of the mountaintop. Similarly, the boundary points of the bottom of the mountains could also be extracted from the above method. In fact, the extracted boundary points are still horizontal distributed, and it should be scanned again from the vertical direction. After the twice scan, the boundary of the altitudinal belt was extracted with the correct format of altitudinal belts.

1.3.3 Altitudinal belt extraction

From the result of the altitudinal belt remote sensing, the horizontal distribution of altitudinal belt information has already achieved. Then, the horizontal information would be transformed to a form of altitudinal belt spectra in this step. A beam raster of NS-trending lines which is parallel to the ground was built at first. After this, DEM was scanned using the NS-trending lines. And then, the positions of the intersection points were recorded. Based on the position records, the altitudinal belt type which is the same position with intersection was also recorded. When the scan was finished, a row of the altitudinal belt spectra at a pre-concerted elevation would come into being.

```
&do i := 1 &to 150 &by 1
tem1 = con(kunlundem >= ( 1400 + %i% * 50)
& kunlundem <= 1450 + %i% * 50, 1, 0)
tem2 = con(tem1 ==1, hdabt)
tem3 = zonalmajority( vbeam, tem2)
tem4 = con(tem5 >= (1400 + %i%*50) & tem5
< (1450 + %i% *50), -1* tem3, tem5)
kill tem1 all
kill tem2 all
kill tem3 all
kill tem5 all
tem5 = tem4
kill tem4 all
&end
```

The above ARC Macro Language (AML) program is a block for scanning once from elevation 1400m to 8900m with a scanning height of 50m. [kunlundem] is the name of the DEM, [hdabt] is the horizontal distribution map of altitudinal belt types, and [vbeam] is the raster of NS-trending beam lines. Using the loop statement, and moving the beam of NS-trending line from the lowest location to the highest location, rows of spectrum would be achieved. Arrayed in turn from the bottom up, the rows of spectrum would form the integrated spectra of altitudinal belt eventually.

1.3.4 Information generalization on the condition of terrain shading

There are obvious limitations of spectral of altitudinal belts in showing the land-cover patterns from lengthwise direction for the sake of data

structure of altitudinal belt spectra. Images of vegetation and land-cover is horizontal two-dimensional data in the spatial distribution, while spectral of altitudinal belt has a data structure of vertical two-dimension. As the adret of Kunlun Mountains is also made up of small massifs, the phenomenon of terrain shading occurs. As a result, the type of altitudinal belt may be disparate in different slope of the massifs, and thus we would get a conflicting result in the same position of the spectra of altitudinal when record from lengthwise direction. Accordingly, a step of information generalization should be taken during the process of altitudinal belt extraction. In this paper, the dominant type of altitudinal belt was taken as the representative belt type. During the altitudinal belt extracting, the frequency of every belt type were calculated at each scan proceeding. Then the type with highest frequency was recorded as the last belt type. Through information generalization, the dominant type of altitudinal belt in a given position was thus ascertained.

## 1.4 Extraction of upper and lower boundaries of altitudinal belts

Since the upper and lower boundaries of the altitudinal belt represent distribution limits of

species, it is widely used in geographic analysis. After the extraction of sequential spectra of altitudinal belts, the upper and lower lines of altitudinal belts could be located subsequently. For each of the altitudinal belts, it is not continuous everywhere, although the integrated spectra of altitudinal belts are spatially sequential. Accordingly, upper and lower lines could not be extracted directly from the transforming of raster to vector. In this paper, we developed a way to extract the upper and lower line through vertical comparing. The extracted spectra of altitudinal belts were overlaid with a raster, which recorded the elevation information and had a vertical structure similarly with the spectra of altitudinal belts. Then within a given interval along the mountain strike direction, the highest and lowest points of a specific altitudinal belt could be located. When all the points were extracted, the upper and lower boundaries would come into being.

2 Results and Discussion

2.1 Remote sensing and accuracy assessment of altitudinal belts

Figure 3 displays the result of altitudinal belts
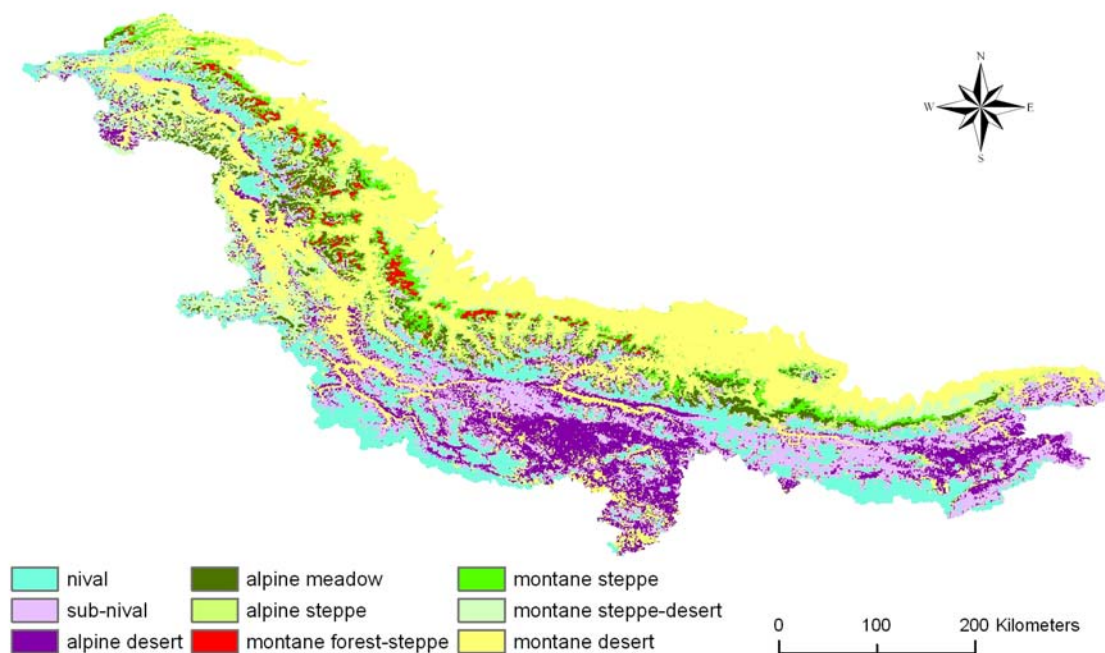
**Figure 3** Horizontal distribution of belt types in west Kunlun Mountains extracted from SPOT-4 VGT-S10 NDVI

remote sensing from data of SPOT-4 VGT-S10 NDVI. According to historical records and field investigations in this area, there are nine types of altitudinal belts: nival, sub-nival, alpine desert, alpine meadow, alpine steppe, montane forest-steppe, montane steppe, montane steppe-desert and montane desert belts. Based on the supervised classification, nine types of altitudinal belts could be identified from the series of images of Mt. West Kunlun. However, the montane forest-steppe belt is very faint, while the other eight of the montane belts are relative distinct. Forest-steppe is now only distributed in few ubac of the west part of Mt. West Kunlun, and it could hardly form a continuous belt in the study area.

In order to assess the accuracy of the classification, random points were selected from the result of altitudinal belt remote sensing. Considering the disproportion among areas of different belt types, the random points were selected respectively from each altitudinal belt

according to the corresponding belt area. According to the accuracy assessment, the total accuracy is 72.23% and the Kappa coefficient is 0.6046. Comparing the result of classification with LandSat-ETM+ images and the vegetation atlas, we found that the alpine desert belt and the mountain desert belt are somewhat mixed. Besides, the area of sub-nival belt is less than that of vegetation atlas. In fact, the sub-nival belt is difficult to locate accurately from remote sensing. Even in field surveys, there is still plenty of confusion concerning the distinguishing of sub-nival belt.

2.2 Geographic unit partition

Figure 4 (a) displays the extracted borderline of the north side of the West Kunlun Mountains. As we known, mountain is not an entire drainage unit, thus the ridge line dividing north side from south side could not be extracted directly through drainage area partition. When the geographic units
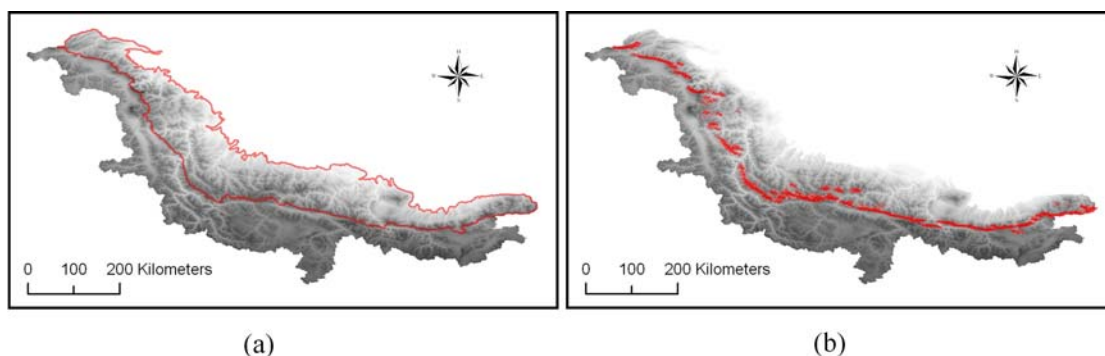
Figure 4 (a) North side of west Kunlun Mountains from geographic unit partition (b) Mountaintops of the north side of west Kunlun Mountains on the north-south direction
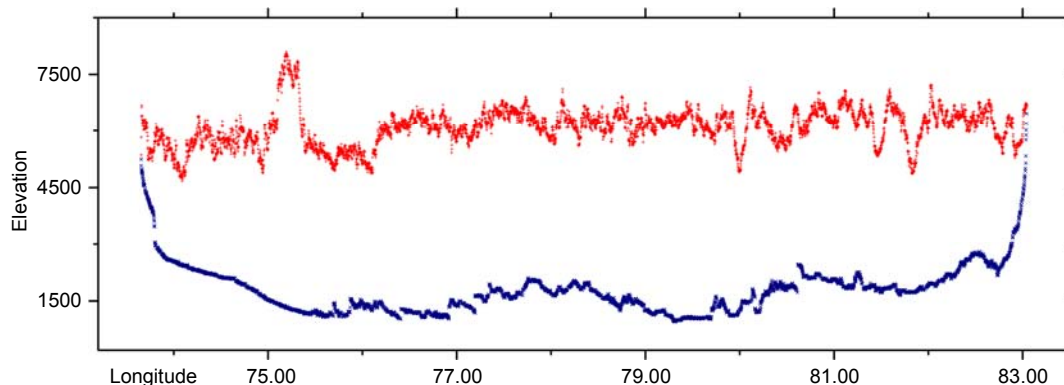
Figure 5 Vertical patterns of the higher points and the lower points which constitute the silhouette line of west Kunlun Mountains

were compartmentalized via hydrologic analysis functions, it is necessary to assemble the geographic units for forming an integrated mountain side according to the geomorphologic structures of Mt. Kunlun. In figure 4 (a), the area rounded red line is the north side of Mt. West Kunlun, which extends from west to east.

2.3 Boundary calculation

Figure 4 (b) shows the recorded highest points which generated from DEM scanning on the north-south direction. The highest points which symbolized with red color were still horizontal distributed. Then, after the second scan from the vertical direction to the ground, the horizontal distributed points were transformed to vertical distributed. As shown by figure 5, the red points are the highest points and the blue points represent the lowest points. All the points constitute the silhouette line of west Kunlun Mountains. Connecting the dispersed points in turn, the edge line of the north block of West Kunlun came into being.

2.4 Altitudinal belt extraction and Information generalization

In this paper, we calculated the altitudinal belt using AML language in ArcGIS. Similarly with the boundary extracting, the altitudinal belts would be extracted through twice scan. During the process of altitudinal belt extracting, there would be a

procedure of information generalization. Considering that the information of montane forest-steppe belt is very faint and important in this area, we toned up its information when generalized the disparate information on the condition of terrain shading. The eventual sequential spectra of altitudinal belts extracted from remote sensing were shown by figure 6. After twice-scan and information generalization, the automatic transition of horizontal maps to vertical belts was realized. Through this way, data of horizontal land-cover of mountains, such as the vegetation maps and the classification results of remotely sensed images, could be all transformed automatically to sequential spectra of digital altitudinal belts.

2.5 Extraction of upper and lower lines of altitudinal belts

Since the sequential spectra of altitudinal belts have been extracted, the upper and lower line of altitudinal belts could be located subsequently. Based on the method discussed in this paper, every altitudinal belt of the spectra could be extracted. Figure 7 (a) and Figure 7 (b) displayed the auto-extracted lower line and upper line of sub-nival belt, while Figure 7 (c) and Figure 7 (d) displayed the upper line and lower line of montane steppe belt. In these figures, the gray lines showed the extracted boundaries of belts, and the black lines are the moving average value of the boundaries. As we known, the upper and lower
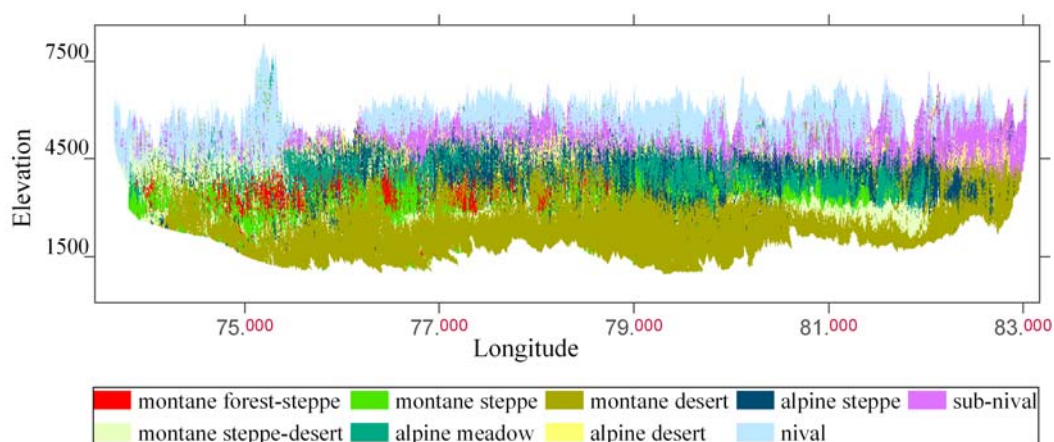
Figure 6 Sequential spectra of altitudinal belts extracted from classification of remotely sensed data
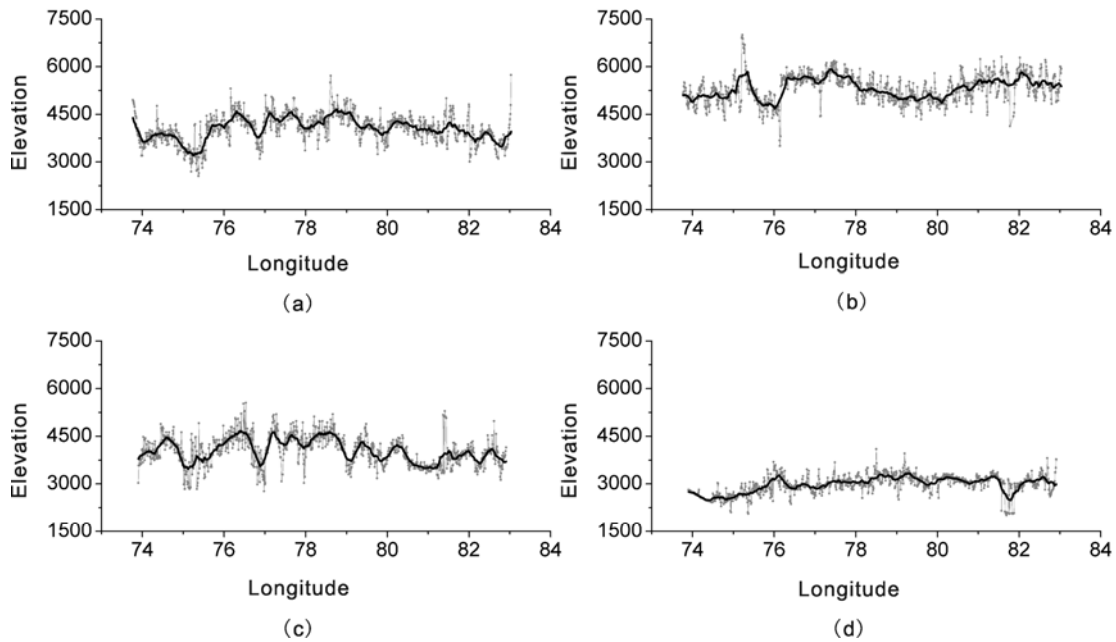
Figure 7 Upper and lower boundaries extraction of altitudinal belts: (a) auto-extracted lower line of sub-nival belt; (b) auto-extracted upper line of sub-nival belt; (c) auto-extracted upper line of montane steppe belt; (d) auto-extracted lower line of montane steppe belt

boundaries represent a tension zone where adjacent altitudinal belts overlap with each other. It is thus difficult to locate the accurate positions of boundaries for each altitudinal belt, and the extracted points in upper and lower lines would be fluctuated within a short distance. Limited by the data accuracy and classification veracity, there would be leaps and mutations in some of the extracted data. Accordingly, the moving average value of the boundaries might be more suitable for analyzing the spatial pattern of altitudinal belts as the equilibrium lines of overlapped zones.

2.6 Relationships between the altitudinal belts based on the montane natural belts concerning vegetation types and the altitudinal belts based on geomorphologic zones

Similar with vertical zonality of vegetations, there are often obvious phenomena of geomorphological altitudinal belts in mountain areas. Due to the great height of the West Kunlun Mountains, geomorphologically recordable altitudinal levels are also especially important in this area.

Both the tectonic activity and the exogenetic process are responsible for the geomorphologic formations, and the geomorphological altitudinal belts are mainly the representation of exogenetic process (MU and TAN 1992). In shaping the geomorphologic formation, climate was one of the most important factors for exogenetic process (Wendland 1996). On different climate conditions, disparate vertical geomorphologic zones including fluvial zone, periglacial zone and glacial zone would be formed by diverse processes such as water erosion, freeze-thaw erosion and glacial erosion, according to the different combinations of exogenetic processes and the different leading processes.

In order to reflecting the geomorphological altitudinal zonality, it is necessary to identify the genetic types of geomorphology. In classical geomorphology, geomorphological classification mainly concerns the demarcation of uniform relief forms (Dikau 1989). However, it is difficult to automatically distinguish geomorphological altitudinal belts directly through geomorphological relief form from remotely sensed images. Traditionally, spatial data of geomorphology distribution have been acquired from the relief

map, and ascertained from field survey. In recent years, supported with expert knowledge and field work, the method of remote sensing image visual interpretation has been used for geomorphological mapping (YAO et al. 2007, XIAO et al. 2008). Despite the fact that nowadays geomorphometric basic attributes such as slope, aspect, profile curvature, ridge, ravine, etc. can be accessed through the spatial analysis of DEM, it is still difficult to design algorithms which could link the relief forms with the geomorphologic genetic types. Because of the complicated relationships between geomorphological forms and geomorphogenesis, there are still scarce of effective ways to realize the automated classification of the genetic types of geomorphology from remotely sensed images according to relief forms directly yet.

Nevertheless, considering that both the geomorphological altitudinal belts and the vegetation altitudinal belts are all delimited by climatic constraints of the altitude, there are possibilities for using vegetation in the characterization of geomorphological forms and processes (Kozlowska and Raczkowska 2002). The distribution of periglacial geomorpholgy in the West Kunlun Mountains depends mainly upon vertical zonation (LI 1987). Vertical extent of present periglacial belt is usually defined by the snow line and the tree line, and the tree line often represents the lower boundary for certain periglacial processes (Washburn 1973, Klose 2006). However, it is not a universal phenomenon. According to the investigation in the Tibetan mountains at 34°50' to 40° N by Kuhle (1985), there is the occurrence of solifluction below the upper timber line. It is also impossible to locate the lower boundary of periglacial belt via tree line in West Kunlun Mountains. Although there are montane forest-steppe belt in this area, the tree line is not consecutive.

Even so, we can find other indicators of the lower boundary of periglacial altitudinal belt in west Kunlun Mountains. In the ordinary course of nature, periglacial altitudinal belt is just above the alpine meadow belt or alpine steppe belt in this area (ZHENG and ZHANG 1989, ZHENG 1999). In some places, the upper line of the montane forest-steppe is still one of the indicators of the lower boundary of periglacial altitudinal belt. From the result of field investigations and the remote sensing visual interpretation, the nival belt is corresponding to the glacial altitudinal belt, and the sub-nival belt belongs to the periglacial altitudinal belt. According to the field investigation by LI (1987) in west Kunlun Mountains, the lower limit of the periglacial geomorphology belt is about 4000m in altitude generally. It is coincident with the digital extracting of sub-nival belt. Below the periglacial altitudinal belt is the fluvial altitudinal belt. Strong weathering and erosion belt could be distinguished above the elevation of 3500 meters. Moreover, loess geomorphy could also be found in some area of the northern slope and piedmont in west Kunlun Mountains. The highest level of the loess geomorphy could reach an elevation of more than 4500 meters above sea-level.

3 Conclusions

In this paper, we discussed a digital method to extract the spectra of altitudinal belts from remotely sensed images and the SRTM DEM in mountain regions. The 1km resolution SPOT-4 vegetation 10-day composite NDVI was selected as the data source to achieve the horizontal distribution of altitudinal belts. Based on supervised classification, nine types of altitudinal belts could be identified from the series of NDVI images of the West Kunlun Mountains. According to the accuracy assessment, the total classification accuracy is 72.23%, and the Kappa coefficient 0.6046. The northern side of the West Kunlun Mountains was compartmentalized via hydrologic analysis functions. A way of twice-scan was subsequently used to realize the automatic transition of horizontal maps to altitudinal belt boundary and vertical belts. Through information generalization in the process of altitudinal belt extracting, conflicts in belt-specifying on the condition of terrain shading were eliminated. Sequential spectra of altitudinal belts were extracted digitally. The upper and lower lines of the altitudinal belts were achieved by vertical scanning of the belts. Finally, the relationships between the altitudinal belts based on the montane natural belts concerning vegetation types and the altitudinal belts based on geomorphologic zones were discussed. In general, even though it still requires further fine tuning, the digital extraction

method presented here is effective at digitally identifying altitudinal belts, and could be helpful in rapid information extraction over large-scale areas.

Acknowledgments

References

Allan, N.J.R. 1986. Accessibility and Altitudinal Zonation Models of Mountains. Mountain Research and Development **6**(3): 185-194.

Becker, A. and Bugmann, H. 1999. Global Change and Mountain Regions: the Mountain Research Initiative. GTOS Report 28. Pp.22.

Berthier, E., Arnaud, Y., Vincent, C., et al. 2006. Biases of SRTM in High-mountain Areas: Implications for the Monitoring of Glacier Volume Changes. Geophysical Research Letters **33**(8): L08502.1-L08502.5.

Böse, M. 2006. Geomorphic Altitudinal Zonation of the High Mountains of Taiwan. Quaternary International **147**:55-61.

Dikau, R. 1989. The Application of a Digital Relief Model to Landform Analysis in Geomorphology. In: Raper, J. (eds.), Three-dimensional Applications in Geographical Information Systems. Taylor & Francis, London. Pp. 51-77.

FENG Jianmeng, WANG Xianping, XU Chongdong, et al. 2006.Altitudinal Patterns of Plant Species Diversity and Community Structure on Yulong Mountains, Yunnan, China. Journal of Mountain Science **24**(1): 110-116. (In Chinese)

Fensholt, R., Rasmussen, K., Nielsen, T.T., et al. 2009. Evaluation of Earth Observation Based Long Term Vegetation Trends – Intercomparing NDVI Time Series Trend Analysis Consistency of Sahel from AVHRR GIMMS, Terra MODIS and SPOR VGT Data. Remote Sensing of Environment. **113**: 1886-1898.

Guglielmin, M., Aldighieri, B., and Testa, B.2003. PERMACLIM: A Model for the Distribution of Mountain Permafrost, Based on Climate Observations. Geomorphology **51**: 245-257.

Hill. R.A., Granica. K., Smith. G.M., et al. 2007. Representation of an Alpine Treeline Ecotone in SPOT 5 HRG Data. Remote Sensing of Environment **110**: 458-467.

HOU Xueyu. 1980. Vertical Patterns of Montane Vegetation in China. In: Vegetation of China. Beijing, China: Science Press. Pp.738-745. (In Chinese)

HOU Xueyu. 2001. The Vegetation Atlas of China (1:1 000 000). Beijing, China: Science Press. Pp. 113-124. (In Chinese)

HUANG Xichou. 1962. Structure Types of Vertical Zones for Temperate Mountains in the Eurasia. In: Proceedings of the National 1960 Geographical Symposium. Beijing, China: Science Press. Pp. 67-74. (In Chinese)

Jarlan, L., Mangiarotti, S., Mougin, E., et al. 2008. Assimilation of SPOT/VEGETATION NDVI Data into a Sahelian Vegetation Dynamics Model. Remote Sensing of Environment **112**: 1381-1394.

JIANG Su. 1964. Vertical Zonation and Horizontal Differentiation of Physical Geography in Western Sichuan and Northern Yunnan. In: China Geography Society. Proceedings of the 1962 Symposium on Physical Regionalization. Beijing, China: Science Press. Pp.62-69. (In Chinese)

Klose, C. 2006. Climate and Geomorphology in the Uppermost Geomorphic Belts of the Central Mountain Range, Taiwan. Quaternary International **147**: 89-102.

Körner C. 1998. A Re-assessment of High Elevation Treeline Positions and their Explanation. Oecologia **115**: 445-459.

Kozlowska, A. and Raczkowska, Z. 2002. Vegetation as a Tool in the Characterization of Geomorphological Forms and Processes: An Example from the Abisko Mountains. Geografiska Annaler **84**:3-4.

Kuhle, M. 1985. Permafrost and Periglacial Indicators on the Tibetan Plateau from the Himalaya Mountains in the South to the Quilian Shan in the North (28-40°N). Zeitschrift für Geomorphologie N.F. **29**(2):183-192.

Kuhle, M. 2007. Altitudinal Levels and Altitudinal Limits in High Mountains. Journal of Mountain Science **4**(1): 024-033.

Kullman, L. and Kjallgren, L. 2006. Holocene Pine Tree-line Evolution in the Swedish Scandes: Recent Tree-line Rise and Climate Change in a Long-term Perspective. BOREAS **35**(1): 159-168.

LI Shude. 1987. Permafrost and Periglacial Phenomena in West Kunlun Mountains of China. Bulletin of Glacier Research **5**:103-109.

LIU Huaxun. 1981. The Vertical Zonation of Mountain Vegetation in China. Acta Geographica Sinica **36**(3):267-279. (In Chinese)

Luedeling, E., Sieber, S. and Buerkert, A. 2007.Filling the Voids in the SRTM Elevation Model: A TIN-based Delta Surface Approach. Journal of Photogrammetry & Remote Sensing **62**: 283-294.

Lunetta, R.S., Knight, J.F., Ediriwickrema, J., et al. 2006. Land-cover Change Detection Using Multi-temporal MODIS NDVI Data. Remote Sensing of Environment **105**(2): 142-154.

MU Guichun and TAN Shukui. 1992. Climatic Geomorphology and Study on an Example of Classification of Climatic Landforms in China. Journal of Hubei University **14**(3): 283-289. (In Chinese)

NIU Wenyuan. 1980. Theoretical Analysis of Physico-geographical Zonation. Acta Geographica Sinica **35**(4): 288-298. (In Chinese)

Olthof, I. and Pouliot, D. 2010. Treeline Vegetation Composition and Change in Canada's Western Subarctic from AVHRR and Canopy Reflectance Modeling. Remote Sensing of Environment **114**:805-815.

PENG Buzhou, Chen FU, and Pu Lijie. 1999. Progress in the Study on Mountainous Vertical Zonation in China. Chinese Geographical Science **9**(4):297-305.

PENG Buzhou, Pu Lijie, Bao Haosheng, et al. 1997. Vertical Zonation of Landscape Characteristic in the Narmjagbarwa Massif of Tibet, China. Mountain Research and Development **17**(1): 43-48.

Rabus, B., Eineder, M., Roth, A., et al. 2003. The Shuttle Radar Topography Mission- a New Class of Digital Elevation Models Acquired by Spaceborne Radar. Journal of Photogrammetry & Remote Sensing **57**: 241-262.

Rodriguez, E., Morris, C.S. and Belz, J.E. 2006. A Global Assessment of the SRTM Performance. Photogrammetric Engineering and Remote Sensing **72**(3): 249-260.

Schmidt, H. and Karnieli, A. 2000. Remote Sensing of the Seasonal Variability of Vegetation in a Semi-arid Environment. Journal of Arid Environments **45**: 43-59.

Schweizer, J. and Kronholm, K. 2007. Snow Cover Spatial Variability at Multiple Scales: Characteristic of a Layer of Buried Surface Hoar. Cold Regions Science and Technology **47**(3): 207-223.

Smith, B. and Sandwell, D. 2003. Accuracy and Resolution of Shuttle Radar Topography Mission Data. Geophysical Research Letters **30**:1467-1470.

Tarnavsky, E., Garrigues, S. and Brown, M.E. 2008. Multiscale Geostatistical Analysis of AVHRR, SPOT-VGT and MODIS Global NDVI Products. Remote Sensing of Environment **112**: 535-549.

Troll, C. 1972. Geoecology of the High-Mountain Regions of Eurasia. Steiner, Wiesbaden. Pp. 60-72.

Wang Q. and Tenhunen, J.D. 2004. Vegetation Mapping with Multitemporal NDVI in North Eastern China Transect. International Journal of Applied Earth Observation and Geoinformation **6**: 17-31.

Washburn, A.L. 1973. Periglacial Processes and Environments. Edward Arnold, London. Pp. 320.

Weiss, J.L., Gutzler, D.s., Coonrod, J.E.A., et al. 2004. Long-term Vegetation Monitoring with NDVI in a Diverse Semi-arid Setting, Central New Mexico, USA. Journal of Arid Environments **58**: 249-272.

Wendland, W.M. 1996. Climate Changes: Impacts on Geomorphic Processes. Engineering Geology **45**: 347-358.

XIAO Fei, ZHANG Baiping, LING Feng, et al. 2008. DEM Based Auto-extraction of Geomorphic Units. Geographical Research **27**(2): 459-466.

XIAO Fei. 2006. Digital Analysis and Simulation of Mountain Environmental Factors in West Kunlun Mountains. PhD thesis, The State Key Lab of Resources and Environmental Information System, Institute of Geographic Science and Natural Resources Research, Chinese Academy of Sciences. Pp.95-98 (In Chinese)

YAO Yonghui, ZHOU Chenghu, SUN Ranhao, et al. 2007. Digital Mapping of Mountain Landforms Based on Multiple Source Data. Journal of Mountain Science **25**(1): 122-128. (In Chinese)

ZHANG Baiping, Mo Shenguo, Wu Hongzhi, et al. 2004. Digital Spectra and Analysis of Altitudinal Belts in Tianshan Mountains, China. Journal of Mountain Science **1**(1): 18-28.

ZHANG Baiping, WU Hongzhi, XIAO Fei, et al. 2006.Integration of Data on Chinese Mountains into a Digital Altitudinal Belt System. Mountain Research and Development **26**(2):163-171.

ZHANG Baiping, ZHOU Chenghu and CHEN Shupeng. 2003. The Geo-info-spectrum of Montane Altitudinal Belts in China. Acta Geographic Sinica **58**(2): 163-171. (In Chinese)

ZHANG Baiping. 2008. Progress in the Study on Digital Mountain Altitudinal Belts. Journal of Mountain Science **26**(1): 12-14. (In Chinese)

ZHENG Du. 1994. The Altitudinal Belts of Vegetation and Regional Differentiation of the Karakorum Mountains. In: Research on Vegetation Ecology. Beijing, China: Science Press. Pp. 93-99. (In Chinese)

ZHENG Du. 1999. Physical-geography of the Karakorum-Kunlun Mountains. Beijing, China: Science Press. Pp.48-95, 126, 139-142. (In Chinese)

ZHENG Du and ZHANG Baiping. 1989. A Study on the Altitudinal Belts and Environmental Problems of the Karakoram and West Kunlun Mountains. Journal of Natural Resources **4**(3): 254-266. (In Chinese)

ZHENG Yuanchang and GAO Shenhuai. 1984. Trial Discussion on the Vertical Natural Zone of the Mountain in West China. Mountain Research **2**(4): 237-244. (In Chinese)

ZHONG Xianghao. 2000. Montology and Chinese Mountain Research. Chengdu, China: Sichuan Science and Technology Press.Pp.217-262. (In Chinese)

Zhou, L., Tucker, C.J., Kaufmann, P.K., et al. 2001. Variation in Northern Vegetation Activity Inferred from Satellite Data of Vegetation Index During 1981 to 1999. Journal of Geophysical Research-Atmospheres **106**(D17): 20069-20083.